IEEE Transactions on Automation Science and Engineering (T-ASE) paper, presented at ICRA 2026, Vienna, Austria.
Cite as T-ASE paper.

Surgeon Supervised Autonomous Surgical System for Oral and Maxillofacial Surgery

Qingchuan Ma, Etsuko Kobayashi, Kazuaki Hara, Junchen Wang, Ken Masamune, Hideyuki Suenaga, and Yubo Fan, *Member, IEEE*

***Abstract*—Oral and maxillofacial surgery (OMS) imposes an increasing workload on even the most experienced surgeons due to long operation time, high skill requirements, limited observation field, constrained workspace, and fast-growing patient population. Robot-assisted OMS is particularly challenging, requiring technological advancements to replicate complex surgical workflows executed by human surgeons and novel working concepts to properly address human-machine relationships. We introduced a Surgeon Supervised Autonomous Surgical System (SSASS) aiming to solve emerging bottlenecks in OMS. SSASS custom develops a deep-learning-assisted virtual planning module, a teeth-based monocular camera navigation module, and a six-degree-of-freedom compact robot module to function as surgeons' auxiliary brain, eye, and hand, respectively. These three modules are further seamlessly integrated to autonomously complete most labor-intensive procedures, while prioritizing surgeons to supervise and be responsible for the overall procedure. Le Fort I experiments on five human head models demonstrated that the surgical results of SSASS closely matched the preoperative plan, with high drilling accuracy and acceptable cutting accuracy under a fundamentally new and significantly simplified surgical workflow. Compared to its existing OMS counterparts, SSASS integrates the latest technologies such as deep learning, medical 3D printing, markerless navigation, virtual reality, and collaborative robotics, providing a comprehensive surgical solution for encompassing the entire OMS loop.**

***Note to Practitioners*—This study was motivated by the increasing needs of automating the surgical procedure of oral and maxillofacial surgery (OMS) to reduce the mismatch between the inadequate number of professional surgeons and the fast-growing patient population. Although more and more surgical hardware and software were introduced into the operating room to assist the surgeon, their workloads are only partially alleviated as surgeons still have to perform many vital procedures manually. This study proposed a Surgeon Supervised Autonomous Surgical System (SSASS) with a significantly simplified workflow for achieving predictable, controllable, and repeatable OMS outcomes. SSASS could avoid many previously necessary analyzing procedures and surgical tools, freeing surgeons from the need to conduct time-consuming manual cephalometric analysis, prefabricate physical surgical models, primary robot programming knowledge or repeatedly program robot trajectory in every surgery, and use physical tracking markers and frequently measure the separated skeleton parts. SSASS introduced a systematical surgical solution aiming to finish most high-workload, tedious, repetitive work while giving the highest priority to surgeons for surveillance. We disclosed key software and hardware information of this system in the manuscript and supplementary materials so that the practitioners could rebuild or improve our current prototype without major difficulties. The experiment results show the high application potential of this system in OMS.**

***Index Terms*—Surgical robot, oral and maxillofacial surgery, navigation, autonomous system, medical device.**

I. Introduction

NEWLY proposed complex surgeries are challenging surgeons' mental and physical limits [1], [2] due to high skill requirements [3], intricate surgical environment [4], and heavy workload [5]. Simply gaining more knowledge and practice may no longer significantly improve surgical outcomes [6]. Accordingly, an increasing number of computer-assisted and robot-assisted technologies are being introduced into the operating room [7]. However, new challenges are accompanied by the rapidly growing intelligence and involvement of novel medical equipment [8], making the relationship between human surgeons and surgical machines a key issue [9]. The questions arising from this developing relationship include the extent to which the machine should be allowed to interfere in surgeries; whether it should be given full decision-making priority during operations; and who should be responsible for operative emergencies.

Received 2 September 2024; revised 19 March 2025 and 24 June 2025; accepted 7 August 2025. Date of publication 2 September 2025; date of current version 5 September 2025. This article was recommended for publication by Associate Editor I. Godage and Editor X. Liu upon evaluation of the reviewers' comments. This work was supported in part by Japan Agency for Medical Research and Development under Grant JP191m0203048h002; in part by Japan Society for the Promotion of Science under Grant JP16K11674, Grant JP19K10258, Grant JP26108008, and Grant PDP20106; in part by the National Natural Science Foundation of China under Grant 52205300, Grant U20A20390, and Grant 12332019; and in part by Beijing Natural Science Foundation under Grant NumberL252078. *(Qingchuan Ma and Etsuko Kobayashi are co-first authors.) (Corresponding authors: Ken Masamune; Hideyuki Suenaga; Yubo Fan.)*

This work involved human subjects or animals in its research. Approval of all ethical and experimental procedures and protocols was granted by the Medical Ethics Committee of the University of Tokyo under Application No. 2553-(3).

Qingchuan Ma and Yubo Fan are with the School of Engineering Medicine, Beihang University, Beijing 100191, China (e-mail: maqingchuan@bmpe.t.u-tokyo.ac.jp; yubofan@buaa.edu.cn).

Etsuko Kobayashi and Kazuaki Hara are with the Graduate School of Engineering, The University of Tokyo, Tokyo 113-8654, Japan (e-mail: etsuko@bmpe.t.u-tokyo.ac.jp; hara@bmpe.t.u-tokyo.ac.jp).

Junchen Wang is with the School of Mechanical Engineering and Automation, Beihang University, Beijing 100191, China (e-mail: wangjunchen@buaa.edu.cn).

Ken Masamune is with the Institute of Advanced Biomedical Engineering and Science, Tokyo Women's Medical University, Tokyo 162-8666, Japan (e-mail: masamune.ken@twmu.ac.jp).

Hideyuki Suenaga is with the Department of Oral-Maxillofacial Surgery and Orthodontics, The University of Tokyo Hospital, Tokyo 113-8655, Japan (e-mail: suenaga-tky@umin.net).

This article has supplementary downloadable material available at https://doi.org/10.1109/TASE.2025.3604891, provided by the authors.

Digital Object Identifier 10.1109/TASE.2025.3604891

IEEE Transactions on Automation Science and Engineering (T-ASE) paper, presented at ICRA 2026, Vienna, Austria.

The complexities of some new surgeries have exceeded the physical limits of human surgeons [10], [11] who show natural disadvantages compared to machines. For example, the human brain requires additional reminding tools to recall complex surgical procedures. Reference [12], the naked human eye cannot see-through the skin to observe the internal organs [13], and human hands become fatigued during overlong surgery [14]. New planning, navigation, and robot technologies remain highly desirable to compensate for human physical limitations [15], [16]. However, it is difficult to realize all human-capable functions due to the challenges in the current state-of-the-art technologies [14], [17]. These two basic facts give rise to the more practical idea of developing artificial substitutes that demonstrate superiority over the human brain, eyes, and hands in specific tasks for analyzation, observation, and execution, rather than the versatility to perform general tasks to match that of humans.

However, focusing on the improvement of individual module's performance will only achieve limited unilateral enhancement. A systematic view must be taken to reconsider the human-machine relationship for fundamental improvement [18]. Many current surgical equipment work independently and treat the surgeon as the connection interface between all modules [19]. In such a surgeon-centered working concept, surgeons are highly involved in every surgical step and their expertise significantly impacts final surgical outcomes [20]. Consequently, the surgeon's workload is partially relieved and human-related factors still negatively affect the predictability, controllability, and repeatability of surgical results [21]. A possible solution is to enable surgeons' independence from the executive loop and improve the integration of the machine. Thus, it will function as an artificial surgeon to perform most of the work with minimal human involvement. However, these increased integrations by reducing the intermedium would come at the expense of exponentially increased technological difficulties inherent to using more custom hardware and software to compensate for human absence [22]. It is difficult even for an experienced surgeon to conduct complex surgery, and developing a surgical system to replace human work introduces more technological challenges [23].

As one of the typical complex surgeries, oral and maxillofacial surgery (OMS) is a discipline that treats patient anatomical defects in the mouth, jaw, face, neck, skull, and surrounding structures [24]. With an increasing group of people choosing OMS for treating diseases and aesthetic purposes. Reference [25], the OMS field is encountering two major challenges. The first challenge relates to the individual surgeon. During OMS, the surgeon completes a series of complex procedures in a narrow working space. The operation was conducted through the patient's mouth or an incision while avoiding damage to many important nerves and blood vessels. Surgeons cannot fully observe the surgical field with the naked eye due to a limited field of view, which is occluded by soft tissue and blurred by blood. A typical OMS may last for eight hours or longer, with additional hours spent to make the surgical plan preoperatively and recall it during surgery [16]. The second challenge is to OMS community. As a large number of patients undertaking OMS each year with the fast-growing population ratio, there is a shortage of qualified surgeons to meet the expanding clinical demand. The career path of the professional OMS surgeon is long and costly. Reference [26], making it difficult to train enough surgeons in a short period. In addition, the surgical outcomes significantly depend on the surgeon's experience, and human-related factors confine the predictable, controllable, repeatable surgical results. Therefore, an autonomous surgical system is highly desirable in OMS to reduce the workload and shrink the surgeon-patient gap for more standardized surgical outcomes.

Nevertheless, achieving a fully autonomous surgical system for OMS is still an overly aggressive goal due to the high surgical risks and the limitations of the state-of-the-art technologies. The autonomy level of robot-assisted surgery (RAS) in OMS is experiencing a steady improvement. According to the level of autonomy (LoA) proposed by Yang et al. [27], current medical robots can be categorized into six different levels. The LoA 0 and 1 are no autonomy and robot assistance, respectively. A typical example at these levels is the da Vinci surgical system [28]. In the OMS field, some LoA 0-1 medical robots have also been proposed based on joint-actuated robotic arm platforms [29] and custom end effectors [19]. We previously developed a custom OMS robot to conduct sagittal split ramus osteotomy (SSRO) and intraoral vertical ramus osteotomy (IVRO) [30]. Although this robot used program-based control rather than a teleoperator, it still belonged to the LoA 1 robot in nature, because the motion trajectory was directly determined by the surgeon. There are also other well-known LoA 2 and 3 surgical systems, such as RoboDoc [31] and Mako [32]. Accordingly, some researchers have also proposed these levels of autonomous OMS systems [33], [34], including our previous work that combined markerless navigation with a compact robot [35], [36]. The system can dynamically change its trajectory according to the patient's head pose, and complete the surgical procedure at the region where surgeons fail to observe using naked eyes. However, the static trajectories of the robot still have to be programmed by the surgeon, and it cannot change the drilling direction according to the topology of the head surface as a human surgeon did. Therefore, in this study, we made major updates to our hardware and software by seamlessly integrating custom planning, navigation, and robot module into a functional system. The system could externalize the surgeon from the main executive loop and autonomously complete the majority of the labor-intensive surgical work. To the best of our knowledge, SSASS is the first functional system in the OMS field that could automate most procedures with a fundamentally new surgical workflow.

The novelties of this study can be summarized into three aspects. First, SSASS enables autonomous completion of most high-workload OMS procedures while allowing surgeons to supervise the overall operation in real-time through virtual reality (VR) images, aiming to achieve a better work distribution relationship between the surgical system and surgeons. Second, SSASS significantly simplified OMS workflow by avoiding many necessary surgical tools and analyzing methods, such as manual cephalometric analysis, prefabricating physical surgical models, mastering robot programming knowledge, and optical tracking markers. Third, SSASS

IEEE Transactions on Automation Science and Engineering (T-ASE) paper, presented at ICRA 2026, Vienna, Austria.

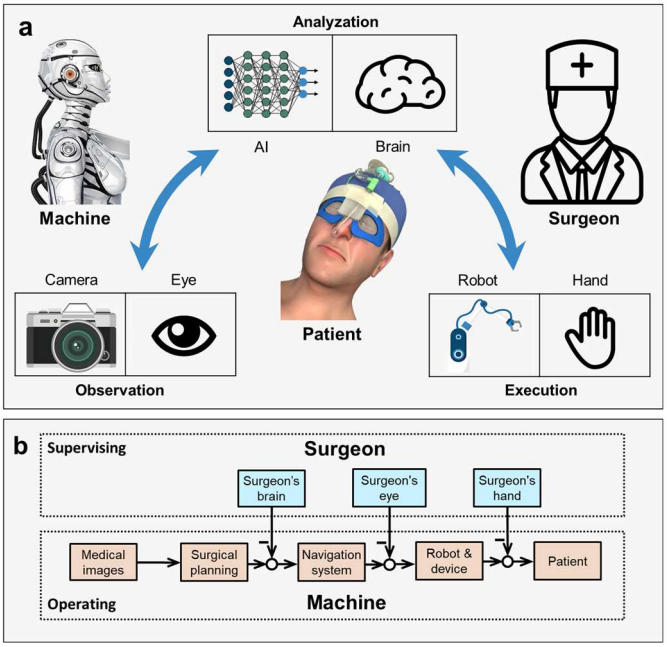

Fig. 1. **General concept**. **a** Relationships between three human organs and corresponding artificial substitutes. **b** Relationships of workload arrangement and working priority between human surgeon and surgical machine. Hereafter, "machine" refer to all types of human-made surgical equipment, devices, and methods used to assist a surgeon's work.

introduced a comprehensive solution encompassing the entire surgical loop, from preoperative planning to intraoperative execution, by leveraging cutting-edge technologies such as deep learning, 3D printing, markerless navigation, virtual reality, and collaborative robotics.

II. Materials and Methods

A. General Concept

Considering the characteristics of OMS and technological difficulties, we propose a surgeon supervised human-machine working concept as shown in Fig. 1. In this working concept, the machine would become the main operator to finish the most tedious and fatiguing work. Meanwhile, the surgeon would work as a benign factor to the system, able to adjust, interfere, and supervise every working step. The machine's workload is heavier than the surgeon's, while the surgeon has a higher priority than the machine. Based on this concept, we developed SSASS by adopting a systematic relationship framework to properly address the key challenges in OMS.

B. Specifications of Each Module

In contrast to the versatile capabilities of the human brain, eye, and hand, the system's planning, navigation, and robot modules were all highly customized to realize the capability of the three respective human organs for tasks specific to OMS.

1) Planning Module: The planning module aims to mimic the surgeon's brain capabilities and reduce the mental burden. The current mainstream planning method in OMS still heavily relies on the surgeon to conduct cephalometric analysis by manually selecting a series of anatomic landmarks to reflect

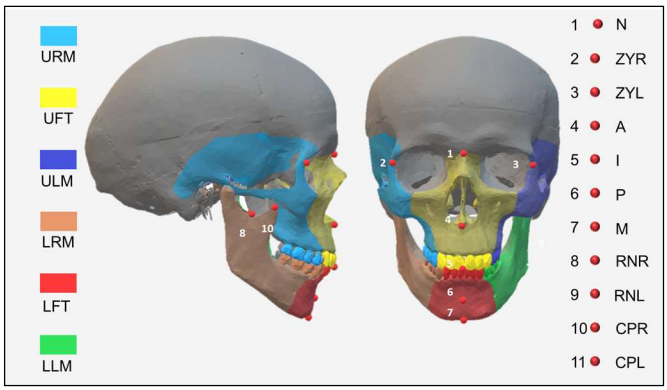

Fig. 2. **Landmark list and teeth group of the head in the coronal and sagittal plane**. The meanings of the abbreviations are listed in Table I.

TABLE I
Abbreviations and Locations of Landmark List and Teeth Group

Bone region	Abbre.	Landmark	Abbre.	Teeth
Skull	N	Nasion	URM	Upper right molars
	ZYL	Zygomatic point left	UFT	Upper front teeth
	ZYR	Zygomatic point right	ULM	Upper left molars
Maxilla	A	Anterior nasal spine	LRM	Lower right molars
	I	Incisors intersecting point	LFT	Lower front teeth
Mandible	P	Pogonion	LLM	Lower left molars
	M	Menton		
Ramus	RNL	Ramus notch left		
	RNR	Ramus notch right		
	CPL	Coronoid process left		
	CPR	Coronoid process right		

the biomechanical features of the patient's head [37]. The surgeon has to repeat this lengthy process for every new patient, which makes the conventional planning method time-consuming and tedious [38]. To address the clinical demands, we automated the preoperative procedure by exploiting the valuable planning skills from both pre-and postoperative computed tomography (CT) images conducted by skilled surgeons.

To quantitatively summarize the key features of the human head, we divided the patient's teeth into six groups and selected eleven anatomical landmarks for locating operative regions and skeletal changes during surgery (Fig. 2, Table I). The six teeth groups represented the corresponding surgical regions. The eleven anatomical landmarks labeled the pre and postoperative movement of five head bones: skull, maxilla, mandible, right ramus, and left ramus. To prepare the training material, patient CT images undertaking the OMS at The University of Tokyo Hospital were screened and labeled by a professional OMS surgeon based on the inclusion criteria. 56 CT data were qualified and subsequently selected, we allocated 50 of them to the training group and 6 of them to the testing group, with each of them equally having 330 slices.

A cascaded convolution neural network (CNN) was trained using both pre and postoperative CT images, which could

IEEE Transactions on Automation Science and Engineering (T-ASE) paper, presented at ICRA 2026, Vienna, Austria.

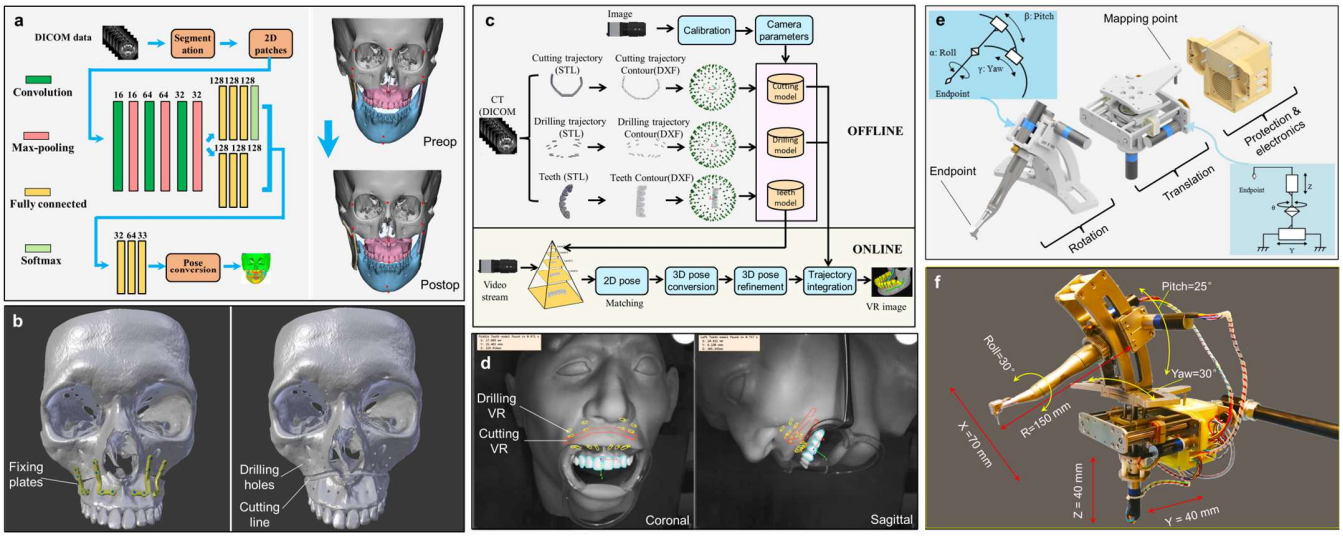

Fig. 3. **Planning, navigation, and robot modules**. **a** Network structure of landmark-based deep learning model for predicting postoperative skeleton changes (left) and one example of model-predicted results (right). **b** Planned postoperative result for 3D printing fixing plate (left) and restored preoperative result for designing robot trajectory (right) using the proposed custom virtual surgery approach. **c** Offline and online workflow of navigation module. **d** Coronal (left) and sagittal (right) virtual reality image taken during online tracking. **e** 3D designing model and mechanical principle of the robot's rotation and translation mechanism. **f** Actual robot image and movement dimension.

automatically extract the aforementioned 11 landmarks from CT images and predict the optimal postoperative landmark changes to assist surgical planning (Fig. 3a). This model used 3-layer CNN blocks to extract the features from 2D patches of CT images, and each block had a standard Conv-BatchNorm-ReLU operation. The extracted feature maps were further fed into two sub-networks with 3 fully connected layers for classification and regression tasks. The data were then inputted into a 3-layer multi-layer perceptron (MLP) to predict the movement of the landmarks after surgery. The model closely mimicked the human surgeon's two-step planning workflow. First, the backbone CNN part located the landmarks from CT images like the surgeon manually drew landmarks, then the MLP part predicted optimal landmark movement like the surgeon moved the skeleton part to make landmarks closer to esthetic standards. Once the model was trained, only preoperative CT images were required and the surgeon could see the postoperative results in 43 seconds. The model's landmark-based inferring results could represent 74.4% of 3D regions at the volume level when compared with the ground truth of human surgeons. With the assistance of this model, surgeons could try as many times as they want and no longer need to prefabricate physical surgical models and repeatedly conduct cephalometric analysis.

Subsequently, the model-predicted result was interpreted using a custom virtual surgery (VS) method with a specialized workflow implemented in 3-Matics (Movie S5), which could automatically generate the digital fixing plate based on the topological features of the patient's skull (Fig. 3b). The VS approach could create the robot trajectory directly, without requiring the surgeon's knowledge of robot programming or reprogramming during each surgery. It could also generate VR models of drilling holes and cutting paths, allowing the surgeon to supervise whether the system is performing the procedure as planned. It also designed the digital fixing plates for preoperative 3D printing according to the topological features of the patient's skull, which frees the surgeon from having to manually bend the titanium plate during surgery, not only reducing maxillary assembly errors and saving time, but also alleviating potential recoil problems frequently happened in conventional methods.

2) Navigation Module: The navigation module aims to augment the surgeon's eye capabilities and reduce visual workload. Current navigation technology in OMS typically uses fiducial markers to track the patient's head pose during surgery [39]. Due to the highly limited workspace and the movable human temporomandibular joint [40], physical markers may become obstacles for the surgeon and navigation accuracy could be compromised because of marker drift. Teeth are the only human bones fixed to the skull and exposed to the environment during OMS. Therefore, we used teeth as natural markers to develop a customized markerless navigation module to reflect the position of the head.

The markerless navigation module comprised two successive working phases (Fig. 3c). In the offline phase, the targeting teeth were segmented from the patient's CT images based on Fig. 2 and generated a five-layer dataset of aspect graphs with various projecting angles using a virtual camera method. In the online phase, the real image from the monocular camera was compared with the five-layer aspect graph of the teeth to find the best match based on a similarity score algorithm [36]. Thereafter, the 6-DOF pose of the head would be obtained in real-time (<1 s) and sent to the robot control algorithm to generate the dynamic trajectory. The hardware of the navigation module included a camera (UI-3370 CP, IDS) with its lens (F:12.5 mm, LM12HC, Kowa) and an adjustable illuminator (Model 96T, AmScope). The camera could achieve 300×300 mm^2 FOV in nearly 250 mm working distance with 2048×2048 pixels resolution.

IEEE Transactions on Automation Science and Engineering (T-ASE) paper, presented at ICRA 2026, Vienna, Austria.

The aspect graphs of the drilling and cutting model were also built offline using a similar method and shared the matched pose matrixes of the teeth to be overlaid onto the camera image as VR for the surgeon's supervision during surgery (Fig. 3d, Movie S2). Thus, the physical markers, bulky optical tracking system, and marker interference and drifting problems are avoided. Surgeons also no longer need to use the glabellar reference screw, draw the physical cutting lines, and keep manually measuring the pose of separated skeletal parts to ensure osteotomy accuracy during surgery. As a result, the efficiency and simplicity of OMS navigation can be significantly improved.

3) Robot Module: The robot module aims to replicate the surgeon's hand capabilities and reduce the manual workload. The human mandible and skull are surrounded by important nerves and vessels, and OMS has to be implemented through the patient's mouth or incision to approach the target area, which imposes a high requirement for the accuracy and safety of the surgical procedure. Some joint-actuated robots have been proposed to conduct OMS based on the reformation of the general robot platform with the customized end effector [41]. Those mechanical forms of robots are not customized for the OMS clinical conditions and their workspaces are often too large, which introduces a risk that the robot's trajectory may invade the unintended area and cause serious consequences.

Therefore, we custom-developed a lightweight and compact robot to meet the harsh surgical requirements of OMS in a limited workspace [30]. The robot used the remote center of motion (RCM) mechanism to form a sphere coordinate that could allow the endpoint of the end effector to retain in the same position regardless of the changes of rotation angle (Fig. 3e), which was particularly desirable in OMS because the surgeon needs to keep the endpoint of the osteotomy device unchanged while adjusting its pose. The robot's novel parallel mechanism used the differential movement between two leading screws and one spur gear to realize the end effector's translational movement with high rigidity.

Compared with the joint-actuated robot whose rotational and translational movements are coupled [42], this 6-DOF robot could achieve precise movement in a highly limited workspace and could make both movements independent (Fig. 3f). Six BLDC motors (Faulhaber 1628 024 B) were used to drive six movement axes, each controlled by the local controller (Faulhaber MCBL 3002P RS) based on the primary-secondary control. Its electromechanical design not only achieved high movement precision and control simplification, but also could effectively protect the subject from any unintended injuries. With a 1.4 kg weight and compact shape, the robot could be easily deployed by one medical staff and save valuable workspace.

C. Integrated System

Although the three aforementioned modules could work independently to assist the surgeon and showed specific advantages compared with the current mainstream method, it was more important and challenging to seamlessly integrate them to function as an artificial surgeon, while still allowing the human surgeon to actively interfere with every major step. Many surgical devices and assisting software have been introduced into OMS, nevertheless, there are clear disconnections between different equipment, and discontinuities of workflow between preoperative and intraoperative phases. The only connection interface, memory, and information processing unit between preoperative work and intraoperative work is the surgeon. In a robot-assisted OMS workflow, the surgeon may rely on the navigation system to identify the patient's head pose, compare it to the preoperative plan, then manually control the robot to finish the surgery. From the initial to the final execution, there are observation errors from the eye, judgment errors from the brain, and maneuver errors from the hands. Consequently, the surgeons themselves become the main error source, which makes surgical results unstandardizable because different equipment depends on surgeons as linking mediums rather than integrating directly.

Therefore, we made adaptations for each above-mentioned modules and created a dynamic data-sharing interface to connect them as a functional system for reducing the human-related factor to a minimum. From the perspective of hardware, the whole system could be divided into two subsystems. The executive subsystem was responsible for the actual surgery, which consisted of the surgical part and mouth retractor part (Fig. 4a, Movie S1). The surgical part performed the surgery as a human surgeon would, and the retractor part could be manually adjusted to control the opening range of the patient's mouth as a human assistant would in a conventional surgery. The supporting subsystem used a custom-developed medical cart to provide power, communication, and calculation support for the executive subsystem. The supporting subsystem could improve the compactness of the executive subsystem by packaging all heavy input-output hardware inside, and enabling the surgeon to easily supervise and interfere with the surgical procedures through two monitors and three layers of control devices (Fig. 4b). Such design took into account both the surgeon and the assistant, as well as the workspace allocation that the system had to cooperate and share the limited space with many types of equipment in the operating room.

The surgical part of the executive subsystem combined the changeable osteotomy devices, the high-resolution monochrome camera, and the robot to conduct the surgery. Different osteotomy devices could be mounted to the robot and initialized with corresponding device markers by reusing the camera navigation without the need for an absolute encoder. The camera, lens, and adjustable illuminator were mounted to a 90-degrees-rotatable aluminum frame to work either in the sagittal or coronal plane according to different surgical tasks. The initial pose of the robot could be freely adjusted and further firmly fixed to the surgical bed by using the locking mechanism of the supporting arm upon reaching the intended surgical site. The mouth retractor setup could adjust the opening range of the patient's mouth through a circular frame with three Langenbeck retractors (Fig. 4a). Three linear adjustment stages were attached to the circular frame to linearly change the position of the Langenbeck retractor and self-locked once the patient's mouth achieved the planned opening range. Thus, the retracting location and opening range

IEEE Transactions on Automation Science and Engineering (T-ASE) paper, presented at ICRA 2026, Vienna, Austria.

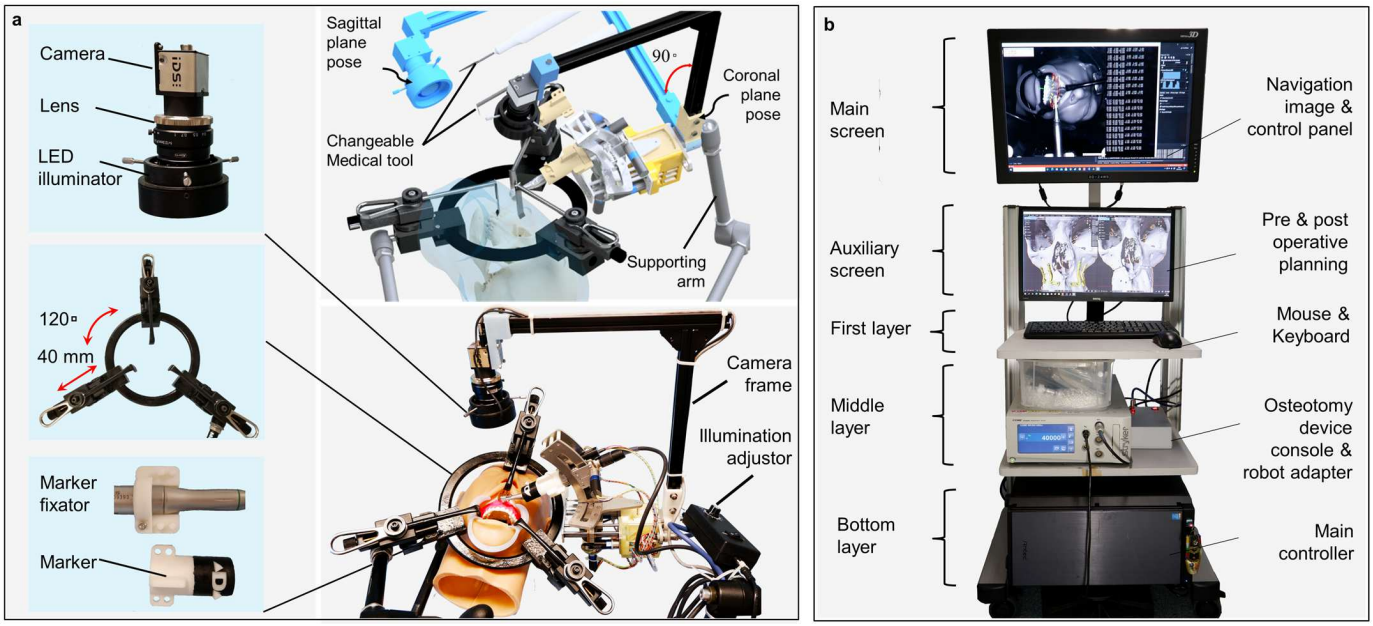

Fig. 4. **Executive part and supporting part of integrated system. a** Designing model and actual picture of the executive subsystem (right) and camera setup, mouth retractor setup, and osteotomy device & its marker (left). **b** Supporting subsystem with screen and layer function allocations.

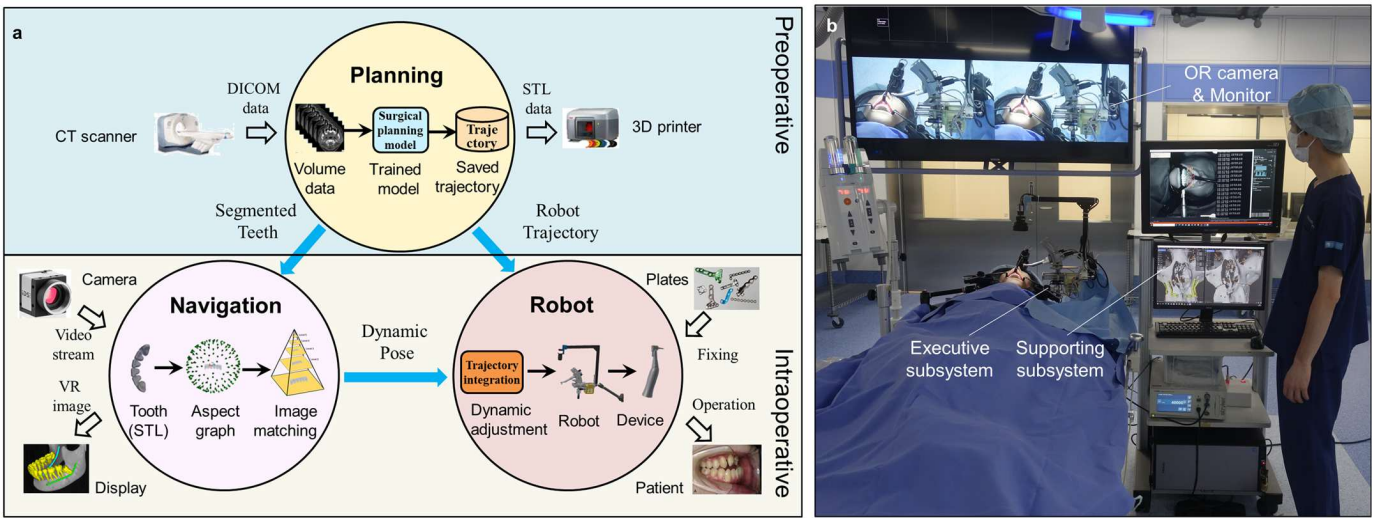

Fig. 5. **Workflow and working environment of integrated system**. **a** The whole system workflow and correlation between modules. Here the blue arrows in the figure indicate the internal data flow, and the hollow arrows indicate external input and output. **b** Actual working picture of the proposed system in operating room, where additional camera and monitor of the operating room are used for auxiliary supervision.

of the patient's mouth could be freely adjusted as a human assistant did (Movie S4).

In the supporting subsystem (Fig. 4b), two monitors were mounted above the first layer, where the main monitor displayed the VR image for the surgeon's surveillance; the auxiliary monitor showed pre- and postoperative surgical plans. The robot adaptor, medical device console (CORE system, Stryker Corp.), and main controller (CPU: Intel Core i7-4820 K, GPU: NVIDIA GeForce GTX TITAN Black) were placed in the remaining layers. The robot adaptor is a custom-made physical interface to connect the robot and the main controller. The supporting subsystem could move freely to the surgical bed and lock its wheels once start the operation.

From the perspective of the data transferring and the workflow, each system module has one external input and one external output with the outside environment and shares the data between modules, as shown by the hollow arrows and blue arrows in Fig. 5a, respectively. The planning module accepted medical images from the CT scanner and output the digital fix plates to the 3D printer, segmented teeth and VR file to the navigation module, and static trajectory to the robot module. The navigation module obtained the video stream from the camera, then output the dynamic trajectory to the robot module, VR image to display. The robot module accepted the 3D-printed fixing plates from the 3D printer and completed the cutting and drilling operation on the patient. In the operating

IEEE Transactions on Automation Science and Engineering (T-ASE) paper, presented at ICRA 2026, Vienna, Austria.

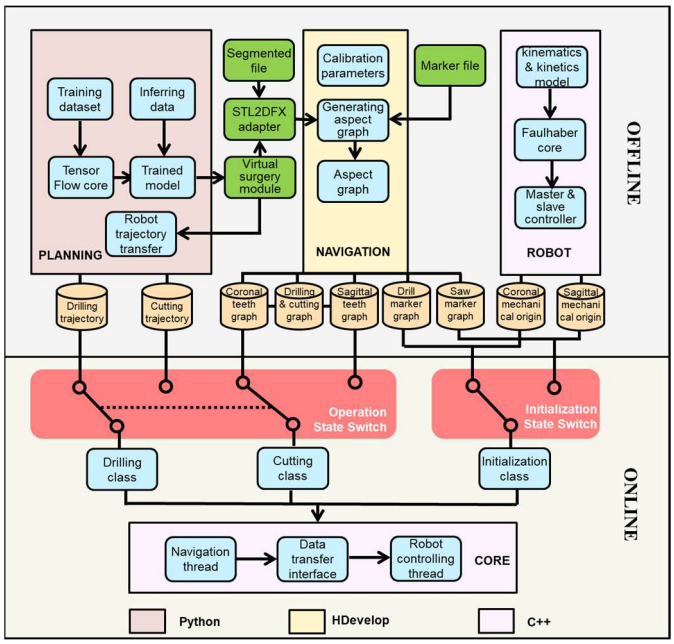

Fig. 6. **Software structures of the whole system.** Different color indicated the programing language used in planning, navigation, and robot module.

TABLE II
MAIN HARDWARE AND SOFTWARE OF THE SYSTEM

Modules	Hardware	Software
Planning	**CPU:** Intel Core i9 CPU (128 GB) **GPU:** 3*NVIDIA Quadro GV100 GPU (96 GB):	Customized network based on Tensorflow-gpu (V 1.9.0). Customized planning approach implemented in 3-Matics (V13)
Navigation	**Camera:** UI-3370 CP, IDS **Lens:** F:12.5 mm, LM12HC, Kowa **LED illuminator:** Model 96T, AmScope	Customized application based on the API of Halcon (V12)
Robot	**Motor**: 6* Faulhaber 1628 024 B **Motor controller:** 6* Faulhaber MCBL 3002P RS **Device controller:** CORE system, Stryker Corp.	Customized application based on the API of Faulhaber
Main controller	**CPU:** Intel Core i7-4820 K CPU (3.7GHz) **GPU:** NVIDIA GeForce GTX TITAN Black GPU	**OS:** Window 10 **IDE:** Visual Studio 2019

room (Fig. 5b), the executive subsystem was placed around the patient's head, while the supporting subsystem was located near the surgeon's side. Additional cameras and monitors of the operating room could be used to show real-time images of the surgical field to check both patient and robot status. After initialization, the system functioned as an artificial surgeon to finish most heavy-duty, tedious, and sophisticated procedures while the human surgeon assisted and supervised the whole process.

The software structures and hardware information are shown in Fig. 6 and Table II and III, respectively. The deep learning model in the surgical planning module was developed based on

TABLE III
ACCESSORY HARDWARE AND SOFTWARE ENVIRONMENT

Hardware	Applications	Software	Applications
CT Scanner: Aquilion ONE ViSION Edition, Canon (Toshiba) Inc. (Resolution:0.351*0.35 1*0.5 mm)	Obtain subjects CT images	**MIMICS** (V 19) + **3-Matics** (V 13), Materialise NV	Segmentation and customized virtual planning
3D Printer: Form2, Formlabs Inc. (Precision: 0.05 mm)	3D print experimental skulls and fixing plates	**Blender** (V 2.79), Blender. Org	Planning results check and showing
3D Scanner: 1) Rexcan CS+, Solutionix Inc. (Precision: 20 um) + 2) Trios3, 3Shape Inc. (Precision: 4.5 um)	3D scan experimental results	**Geomagic Control X** (3D Systems Corp.)	3D comparison between experimental and planning results

TABLE IV
SUBJECTS PERSONAL INFORMATION OF FIVE SKELETAL MODELS IN EXPERIMENT

	Case 1	Case 2	Case 3	Case 4	Case 5
Sex (M/F)	Male	Female	Female	Male	Male
Age (Year)	18Y	18Y	21Y	18Y	19Y
Weight (kg)	85	49	60	58	69

Tensorflow using Python. The navigation module was written using the Halcon platform, and its online part was converted into C++ for dynamic tracking. The control algorithm of the robot module was written in C++ based on the API of Faulhaber. All the offline data was created in advance before operations. The online core of the system was written in C++ and divided into the navigation and robot threads using a custom data share interface. State switch mechanisms were included to control input data and working modes for changing system status and surgical types. The system software was developed in Visual Studio 2019 and implemented in Windows 10.

III. EXPERIMENTS AND RESULTS

A. Experiment Setting

Le Fort I maxillary osteotomy is a challenging treatment in OMS and could be the preferred option for skill testing, because it involves three major procedures in a single treatment (Movie S3). First, drill the screw holes in the maxilla, then cut the bone to separate, and finally fix the maxilla to a planned new potion using the fixing plates [25]. To evaluate the actual performance of the system, Le Fort I was performed on five different models created from the CT scans of real patients (Table IV). Custom virtual surgery was performed on each CT volume based on the predicted results from the deep-learning-assisted planning model to generate four digital L-shaped plates with four holes (d=2 mm). The 3D printing material of the head model and fixing plates created for the experiment was Formlabs White Resin V4. The drilling operation was

IEEE Transactions on Automation Science and Engineering (T-ASE) paper, presented at ICRA 2026, Vienna, Austria.

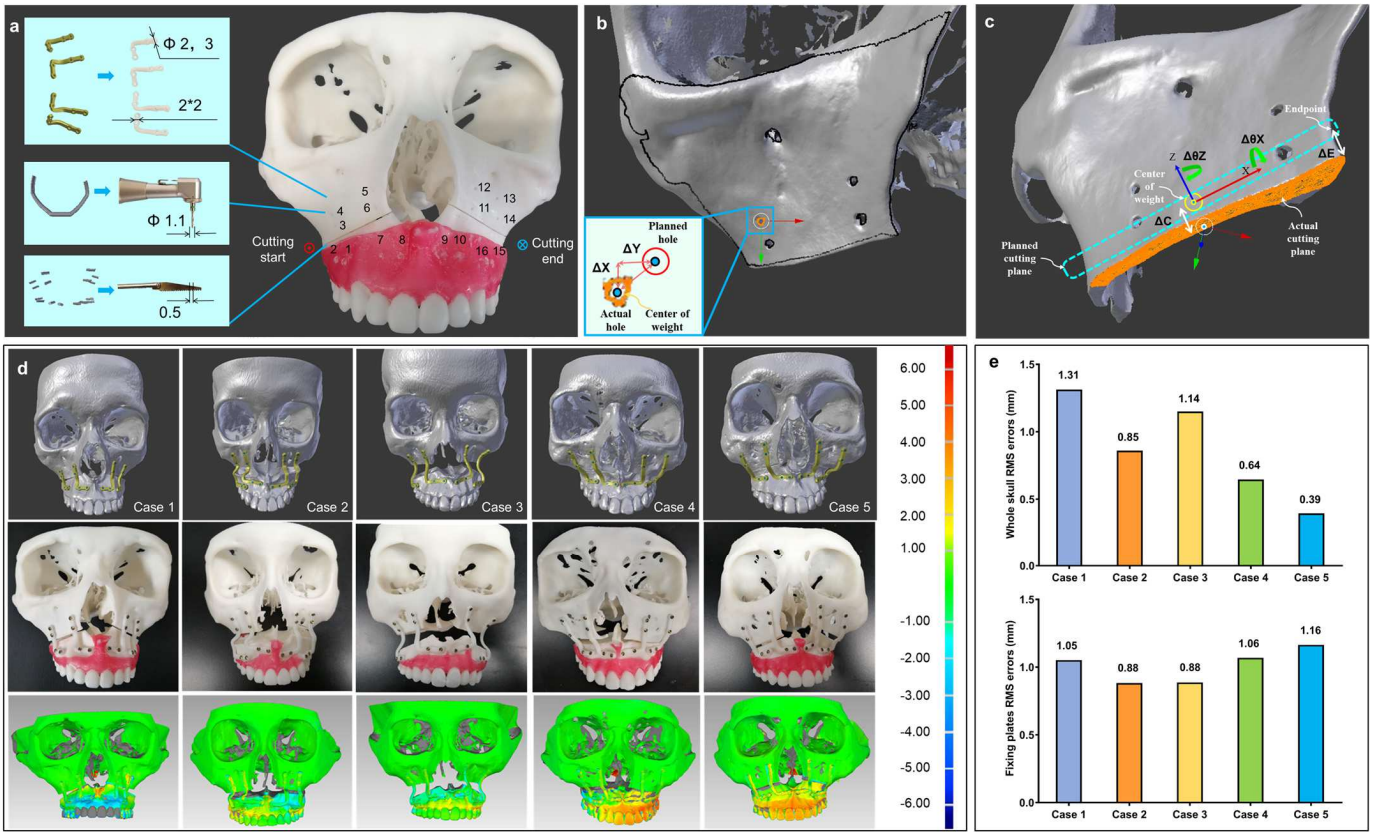

Fig. 7. **Experiments results. a** Actual model after drilling and cutting operation (before separation) and designed drilling and cutting sequence with corresponding tools. **b** 3D-scanned drilling results and corresponding analyzing methods of drilling holes. **c** 3D-scanned cutting results and corresponding analyzing method of cutting planes. **d** Planned(top), actual (middle) surgical model and their 3D comparison (bottom). **e** Comparison results of whole model (top) and fixing plates (bottom) in each case.

implemented using a 1.1-mm drill with the planned 6-DOF pose in the sequence shown in Fig. 7a. The digital drilling holes from the planning module were used to generate VR drilling images and extract the 6-DOF pose to directly guide the robot's drilling movement without manual programming. The cutting trajectory was planned to generate cutting VR images and directly create the robot's movement path. The cutting procedure was finally conducted by the robot using a 0.5-mm thick cutting saw. Subsequently, the maxilla was separated and relocated to the planned new position by fixing plates using 1.1-mm dental screws.

B. Data Acquisition and Processing

Patient CT images were obtained by using a Canon (Toshiba) CT scanner (Aquilion ONE ViSION Edition, resolution: 0.351*0.351*0.5 mm), and were further processed using MIMICS (V19) and 3-Matics (V13) for segmentation and implemented the customized virtual planning method. The patients' head models and corresponding custom fixing plates were made by using a Formlabs 3D printer (Form2, precision: 0.05 mm). Red vax was attached around the alveolar process for functioning as the human gingiva. A 3D scanner from Solutionix (Rexcan CS+, Precision: 20 um) was used to obtain 3D images of experimental head models, and the refining scan was conducted on the teeth parts using a high-resolution scanner from 3Shape (Trios3, precision: 4.5 um). The open-source 3D image processing software Blender (V2.79) was used to check and show the planned surgical result before surgery, and was further used to obtain the barycenters of the drilling holes and to extract the cutting plane from the experimental models after surgery. The scanned experimental head models and planned surgical results were compared using the commercial 3D analyzing software Geomagic ControlX (3D Systems Corp.) for calculating the overall surgical errors. The study was approved by the Medical Ethics Committee of the University of Tokyo (No. 2553-(3)).

C. Results Analysis

The drilling accuracy was analyzed by comparing the experimental centers of weight with the planned hole locations (Fig. 7b). Compared with our previous research and other similar robot-assisted drilling approaches, the drill head in the current study was able to adjust its direction according to the patient's skeleton topology and moved along the normal directions of the bone. Thus, the tangential component of the drilling force could be reduced to a minimum and alleviate the slide of the drill head to reduce the drilling error (Fig. 8a). The X and Y translation accuracies of each case are shown in Fig. 8d, with overall averages of 0.7 ± 0.1 mm and 0.5 ± 0.1 mm, respectively. The relationships between drilling errors and the robot's actual translational and rotational movement were also analyzed. The results indicated a

IEEE Transactions on Automation Science and Engineering (T-ASE) paper, presented at ICRA 2026, Vienna, Austria.

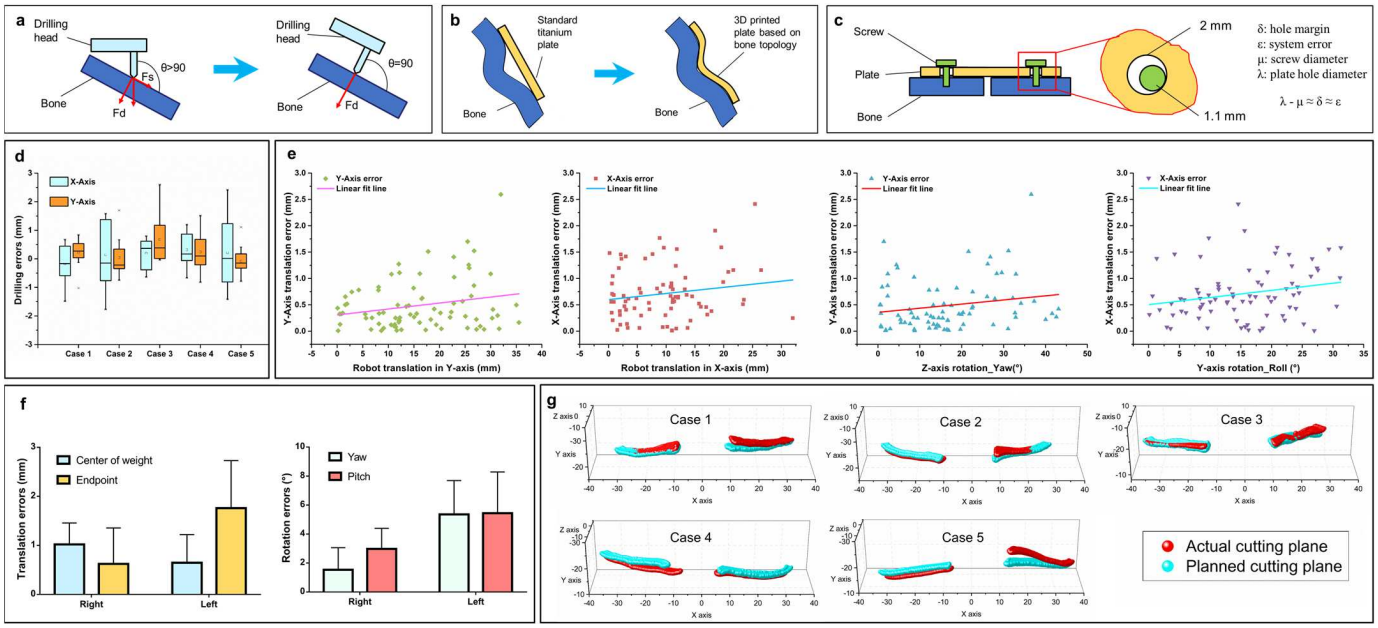

Fig. 8. **Analysis and comparison of experiments results. a** Comparison the drilling operation between conventional approach of directly drilling and the proposed approach of adjusting drilling head according to the bone topology. **b** Comparison of plate fixation operation between the conventional approach of using standard titanium plate and the proposed approach of using 3D printed plated based on the bone topology. **c** Counteract effect of assembling error where a 0.9 mm hole margin was designed to reduce inter-hole and inter-plate errors. **d** Drilling errors of each case. **e** Relationship between drilling errors and translation (first two pictures) & rotation (last two pictures) of robot's actual movement. **f** Translation (left) and rotation (right) errors of cutting plane. **g** Comparison between planned and actual cutting planes in each case.

linear relationship (Fig. 8e) with the slope and R-Square for X translation, Y translation, yaw, and roll are: (1.2E-2 mm/mm, 1.1E-2 mm/mm, 0.8E-2 mm/degree, and 1.4E-2 mm/degree) and (2.8E-2, 5.2E-2, 3.7E-2, and 4.8E-2), respectively. Results showed that improving the mechanical stiffness of the robot and selecting relatively flat surfaces of the skull would have a positive effect on the further improvement of drilling accuracy, as it will reduce the movement range of the drill head to reduce the operation errors.

The cutting accuracy was analyzed by comparing the center of weight offset and endpoint offset between the planned and the actual cutting plane, as well as their yaw and pitch errors (Fig. 7c, Fig. 8 fg). The average offset of the center of weight and endpoint were 0.2 ± 0.4 mm and 0.6 ± 0.7 mm, respectively. The average yaw and pitch errors were $3.4 \pm 1.5°$ and $4.2 \pm 1.6°$, respectively. Larger deviations in the total and obvious inconsistencies between the left and right cutting planes were observed. The possible reason for the performance difference between the two directions could be the error-accumulating effect in the cutting trajectory. Therefore, a predictable improvement could be proposed by dividing the planned cutting trajectory into two parts and setting the start and endpoints to the outer side of each part and the vomer region, respectively.

The accuracy of the whole model assembly was analyzed by 3D-scanning the experimental head model and comparing with the planned surgical results (Fig. 7d). The average RMS error of the whole models and the fixing plates were 0.9 ± 0.2 mm and 1.0 ± 0.1 mm (Fig. 7e). The high assembly accuracy could be attributed to the error-counteracting effect of the inter-hole and inter-plate. In conventional clinical methods, surgeons assemble separated bone parts using standard titanium plates and manually bend them to an intended shape, which is time-consuming and fails to match the surface curve of the patient's head bone. In contrast, the proposed study generated the digital fixing plate to closely contact the bone in most connecting areas rather than only around the plate's holes (Fig. 8b), achieving a better binding surface with the skull. The custom plates were 3D-printed before surgery, which accelerated the surgical procedure by transferring intraoperative work to preoperative work. In addition, there was a 0.9-mm margin between the plate hole (2 mm) and the drill (1.1 mm), which was specially designed to counteract mechanical drilling and skull assembling errors. The 0.9-mm is close to the system's mechanical error (<1 mm). In our preliminary evaluation, such a margin resulted in the inter-hole and inter-plate error reduction (Fig. 8c). This feature benefited a firm assembly and reduced the recoil problem common in conventional OMS.

IV. Discussion

The experimental results are promising for the practical clinical application of the proposed system. Compared with conventional OMS, SSASS proposes a fundamentally new and significantly simplified OMS workflow (Movie S3). The total surgical time could be reduced to no more than two hours even both the preoperative planning and intraoperative operation combined. This is a significant time reduction compared to conventional surgeon-performed OMS, where the intraoperative operation alone can exceed eight hours. The improved surgical efficiency benefited from the avoidance of many surgical tools and analytical methods due to the high integration level [24]. In the preoperative phase, the surgeon

IEEE Transactions on Automation Science and Engineering (T-ASE) paper, presented at ICRA 2026, Vienna, Austria.

does not need to conduct time-consuming cephalometric analysis, prefabricate surgical models, and custom-made surgical splints. In the intraoperative phase, surgeons do not need to draw cutting lines and measure the planned drilling position to reconfirm the correctness of surgical movement. They also do not need to hold the osteotomy tools for a long time as the surgical movement will be finished autonomously by the robot, thereby reducing surgeon fatigue and ensuring that the outcome is consistent with the surgical plan. Some surgical steps can be avoided, such as using surgical splints and wires to fix the maxilla to the mandible, bending the titanium plates during surgery, and using the glabellar reference screw as the fixed skeletal marker. Consequently, surgical time may also be markedly reduced, relieving the surgeons' workload and reducing patients' pain during surgery, thus minimizing the risk of surgical failure due to overlong surgical time.

SSASS's general concept was proposed based on two facts: machines are not yet capable of replicating the versatility of humans under the current state-of-the-art surgical technology; humans show inferior performance compared with machines at specific surgical tasks. SSASS draws upon the merits of both humans and machines to offset their respective weaknesses and form a functional system. Compared with surgeon-centered (robot-assisted) surgical systems such as da Vinci [28], RoboDoc [31], and Mako [32], SSASS externalizes the surgeon from the main executive loop by directly connecting each module to reduce the influence of human-related factors on the system. Nevertheless, SSASS is not a fully autonomous surgical system, which not only unnecessarily increases the technological complexity and wastes the existing human physical capabilities, but also makes the surgical responsibility unclear [27]. SSASS still permits the surgeon to interactively inspect each surgical step, which confers additional reliability by fully exploiting the human's higher intelligence to dynamically interfere with the system, and also retains the surgeon's responsibility for addressing ethical issues.

SSASS introduced a seamless surgical solution to cover the entire surgical loop, rather than utilizing individual tools, devices, and methods for planning [12], navigation [13], and robotic surgery [14]. An advantage was that more integrations meant fewer intermedia were needed to connect each part, which could improve the whole workflow efficiency. However, new working concepts and highly customized hardware and software were required to replace human surgeons' work, which could significantly increase the difficulty of system development. This not only necessitates technical breakthroughs for each module because the research goal can hardly be achieved if we still use the existing technologies, but also the adoption of a systematic view to integrate all modules to target the full lifecycle of a surgery. Although the current prototype shows many capabilities, there are still many aspects that can be improved upon, such as creating a graphical user interface to reduce the learning curve of surgeons, reducing the software scale, and improving the robot's mechanical maturity (Movie S1). Nevertheless, SSASS already demonstrates the possibility and advantage of this idea, and the potential surgical improvements it can convey outweigh the technological barriers it faces. Improved integration and externalizing the surgeon from the main executive loop could represent a new answer to emerging complex surgeries, worth being applied to more surgical modalities.

V. Conclusion

This study proposed a surgeon supervised autonomous surgical system by seamlessly integrating planning, navigation, and robot to complete the OMS procedure under the supervision of a human surgeon. Compared with existing surgeon-centered robotic systems, SSASS could autonomously finish most high-workload surgical procedures with minimal surgeon's direct involvement. The main contribution of the study is to provide a systematic solution to cover the overall OMS workflow, rather than the individual planning, navigation, and robotic equipment merely for limited unilateral enhancement. SSASS achieved a balance between technological advancement and human capability, mental and manual burden, preoperative work and intraoperative work, surgical workload and surgical responsibility, aiming to achieve a better relationship between the surgeon, machine, and patient for better surgical outcomes.

Acknowledgment

The authors would like to thank Ryota Matsubara, Bowen Fan, Izumu Hosoi, Ukyou Yagyuu, Yawu Long, and Koudai Shiuchi for their contributions to code testing, material preparation, and experiment assistance.

References

[1] H. Saeidi et al., "Autonomous robotic laparoscopic surgery for intestinal anastomosis," *Sci. Robot.*, vol. 7, no. 62, Jan. 2022, Art. no. eabj2908.
[2] M. J. Connor, P. Dasgupta, H. U. Ahmed, and A. Raza, "Autonomous surgery in the era of robotic urology: Friend or foe of the future surgeon?," *Nature Rev. Urol.*, vol. 17, no. 11, pp. 643–649, Nov. 2020.
[3] A. Shademan, R. S. Decker, J. D. Opfermann, S. Leonard, A. Krieger, and P. C. W. Kim, "Supervised autonomous robotic soft tissue surgery," *Sci. Transl. Med.*, vol. 8, no. 337, May 2016, Art. no. 337ra64.
[4] J. Sandoval, M. A. Laribi, J. P. Faure, C. Brèque, J. P. Richer, and S. Zeghloul, "Towards an autonomous robot-assistant for laparoscopy using exteroceptive sensors: Feasibility study and implementation," *IEEE Robot. Autom. Lett.*, vol. 6, no. 4, pp. 6473–6480, Oct. 2021.
[5] T. Haidegger, "Autonomy for surgical robots: Concepts and paradigms," *IEEE Trans. Med. Robot. Bionics*, vol. 1, no. 2, pp. 65–76, May 2019.
[6] K. Yu, A. L. Beam, and I. S. Kohane, "Artificial intelligence in healthcare," *Nat. Biomed. Eng.*, vol. 2, no. 10, pp. 719–731, 2018.
[7] I. Andras et al., "Artificial intelligence and robotics: A combination that is changing the operating room," *World J. Urol.*, vol. 38, no. 10, pp. 2359–2366, Oct. 2020.
[8] S. O'Sullivan et al., "Legal, regulatory, and ethical frameworks for development of standards in artificial intelligence (AI) and autonomous robotic surgery," *Int. J. Med. Robot. Comput. Assist. Surg.*, vol. 15, no. 1, Feb. 2019, Art. no. e1968.
[9] Y. Liu, Z. Li, H. Liu, and Z. Kan, "Skill transfer learning for autonomous robots and human–robot cooperation: A survey," *Robot. Auto. Syst.*, vol. 128, Jun. 2020, Art. no. 103515.
[10] B. Mazzolai and C. Laschi, "A vision for future bioinspired and biohybrid robots," *Sci. Robot.*, vol. 5, no. 38, Jan. 2020, Art. no. eaba6893.
[11] O. Elhage, B. Challacombe, A. Shortland, and P. Dasgupta, "An assessment of the physical impact of complex surgical tasks on surgeon errors and discomfort: A comparison between robot-assisted, laparoscopic and open approaches," *BJU Int.*, vol. 115, no. 2, pp. 274–281, Feb. 2015.
[12] D. M. Steinbacher, "Three-dimensional analysis and surgical planning in craniomaxillofacial surgery," *J. Oral Maxillofacial Surg.*, vol. 73, no. 12, pp. S40–S56, Dec. 2015.

[13] L. Jud et al., "Applicability of augmented reality in orthopedic surgery—A systematic review," *BMC Musculoskeletal Disorders*, vol. 21, no. 1, pp. 1–13, Dec. 2020.

[14] H.-H. Liu, L.-J. Li, B. Shi, C.-W. Xu, and E. Luo, "Robotic surgical systems in maxillofacial surgery: A review," *Int. J. Oral Sci.*, vol. 9, no. 2, pp. 63–73, Jun. 2017.

[15] L. Qian, J. Y. Wu, S. P. DiMaio, N. Navab, and P. Kazanzides, "A review of augmented reality in robotic-assisted surgery," *IEEE Trans. Med. Robot. Bionics*, vol. 2, no. 1, pp. 1–16, Feb. 2020.

[16] X. Chen, L. Xu, Y. Sun, and C. Politis, "A review of computer-aided oral and maxillofacial surgery: Planning, simulation and navigation," *Expert Rev. Med. Devices*, vol. 13, no. 11, pp. 1043–1051, Nov. 2016.

[17] C. Bergeles and G.-Z. Yang, "From passive tool holders to microsurgeons: Safer, smaller, smarter surgical robots," *IEEE Trans. Biomed. Eng.*, vol. 61, no. 5, pp. 1565–1576, May 2014.

[18] S. Kumar, C. Savur, and F. Sahin, "Survey of human–robot collaboration in industrial settings: Awareness, intelligence, and compliance," *IEEE Trans. Syst., Man, Cybern., Syst.*, vol. 51, no. 1, pp. 280–297, Jan. 2021.

[19] X. Kong, X. Duan, and Y. Wang, "An integrated system for planning, navigation and robotic assistance for mandible reconstruction surgery," *Intell. Service Robot.*, vol. 9, no. 2, pp. 113–121, Apr. 2016.

[20] M. Kranzfelder et al., "Toward increased autonomy in the surgical OR: Needs, requests, and expectations," *Surgical Endoscopy*, vol. 27, no. 5, pp. 1681–1688, May 2013.

[21] T. B. Sheridan, "Human–robot interaction: Status and challenges," *Hum. Factors*, vol. 58, no. 4, pp. 525–532, 2016.

[22] M. Attia, M. Hossny, S. Nahavandi, M. Dalvand, and H. Asadi, "Towards trusted autonomous surgical robots," in *Proc. IEEE Int. Conf. Syst., Man, Cybern. (SMC)*, Miyazaki, Japan, Oct. 2018, pp. 4083–4088.

[23] E. Battaglia, J. Boehm, Y. Zheng, A. R. Jamieson, J. Gahan, and A. M. Fey, "Rethinking autonomous surgery: Focusing on enhancement over autonomy," *Eur. Urol. Focus*, vol. 7, no. 4, pp. 696–705, Jul. 2021.

[24] D. A. Mitchell, *An Introduction to Oral and Maxillofacial Surgery*. Boca Raton, FL, USA: CRC Press, 2014.

[25] R. J. Fonseca, *Oral and Maxillofacial Surgery-E-Book: 3-Volume Set*. Amsterdam, The Netherlands: Elsevier, 2017.

[26] R. Isaac, D. Ramkumar, J. Ban, and M. Kittur, "Can you afford to become an oral and maxillofacial surgeon?," *BMJ*, vol. 352, p. 163, Jan. 2016.

[27] G.-Z. Yang et al., "Medical robotics—Regulatory, ethical, and legal considerations for increasing levels of autonomy," *Sci. Robot.*, vol. 2, no. 4, Mar. 2017, Art. no. eaam8638.

[28] P. Gomes, "Surgical robotics: Reviewing the past, analysing the present, imagining the future," *Robot. Comput.-Integr. Manuf.*, vol. 27, no. 2, pp. 261–266, Apr. 2011.

[29] J. Zhang et al., "A novel single-arm stapling robot for oral and maxillofacial surgery—Design and verification," *IEEE Robot. Autom. Lett.*, vol. 7, no. 2, pp. 1348–1355, Apr. 2022.

[30] K. Hara, Q. Ma, H. Suenaga, E. Kobayashi, I. Sakuma, and K. Masamune, "Orthognathic surgical robot with a workspace limitation mechanism," *IEEE/ASME Trans. Mechatronics*, vol. 24, no. 6, pp. 2652–2660, Dec. 2019.

[31] A. P. Schulz et al., "Results of total hip replacement using the robodoc surgical assistant system: Clinical outcome and evaluation of complications for 97 procedures," *Int. J. Med. Robot. Comput. Assist. Surg.*, vol. 3, no. 4, pp. 301–306, Dec. 2007.

[32] J. Lin, S. Yan, Z. Ye, and X. Zhao, "A systematic review of MAKO-assisted unicompartmental knee arthroplasty," *Int. J. Med. Robot.*, vol. 16, no. 5, pp. 1–7, 2020.

[33] S.-Y. Woo et al., "Autonomous bone reposition around anatomical landmark for robot-assisted orthognathic surgery," *J. Cranio-Maxillofacial Surg.*, vol. 45, no. 12, pp. 1980–1988, Dec. 2017.

[34] P. Ahmad et al., "Dental robotics: A disruptive technology," *Sensors*, vol. 21, no. 10, p. 3308, May 2021.

[35] Q. Ma et al., "Development and preliminary evaluation of an autonomous surgical system for oral and maxillofacial surgery," *Int. J. Med. Robot. Comput. Assist. Surg.*, vol. 15, no. 4, Aug. 2019, Art. no. e1997.

[36] Q. Ma et al., "Autonomous surgical robot with camera-based markerless navigation for oral and maxillofacial surgery," *IEEE/ASME Trans. Mechatronics*, vol. 25, no. 2, pp. 1084–1094, Apr. 2020.

[37] J. Montúfar, M. Romero, and R. J. Scougall-Vilchis, "Automatic 3-dimensional cephalometric landmarking based on active shape models in related projections," *Amer. J. Orthodontics Dentofacial Orthopedics*, vol. 153, no. 3, pp. 449–458, Mar. 2018.

[38] Q. Ma et al., "Machine-learning-based approach for predicting postoperative skeletal changes for orthognathic surgical planning," *Int. J. Med. Robot. Comput. Assist. Surg.*, vol. 18, no. 3, Jun. 2022, Art. no. e2379.

[39] J. Wang et al., "Augmented reality navigation with automatic marker-free image registration using 3-D image overlay for dental surgery," *IEEE Trans. Biomed. Eng.*, vol. 61, no. 4, pp. 1295–1304, Apr. 2014.

[40] N. Navab, S.-M. Heining, and J. Traub, "Camera augmented mobile C-arm (CAMC): Calibration, accuracy study, and clinical applications," *IEEE Trans. Med. Imag.*, vol. 29, no. 7, pp. 1412–1423, Jul. 2010.

[41] Z. Cao et al., "Pilot study of a surgical robot system for zygomatic implant placement," *Med. Eng. Phys.*, vol. 75, pp. 72–78, Jan. 2020.

[42] R. He, Y. Zhao, S. Yang, and S. Yang, "Kinematic-parameter identification for serial-robot calibration based on POE formula," *IEEE Trans. Robot.*, vol. 26, no. 3, pp. 411–423, Jun. 2010.

Qingchuan Ma received the M.E. and Ph.D. degrees in mechanical engineering from Tsinghua University, Beijing, China, in 2014 and 2017, respectively.

He has been a Visiting Scholar at the Helmholtz-Institute, RWTH Aachen, Aachen, Germany, from 2015 to 2016. From 2017 to 2021, he was a Post-Doctoral Researcher and a JSPS Scholar at the Department of Precision Engineering, The University of Tokyo, and the Department of Oral-Maxillofacial Surgery and Orthodontics, The University of Tokyo Hospital, Tokyo, Japan. He is currently an Associate Professor with the School of Engineering Medicine, Beihang University, Beijing. His research interests include medical robotics, powered exoskeletons, and bionic-inspired joint actuator. He is a Youth Committee Member of Chinese Society of Biomedical Engineering.

Etsuko Kobayashi received the B.S., M.S., and Ph.D. degrees in precision machinery engineering from The University of Tokyo, Tokyo, Japan, in 1995, 1997, and 2000, respectively.

From 2000 to 2003, she was a Research Associate at the School of Frontier Science, The University of Tokyo, where she was a Lecturer from 2003 to 2006. From 2006 to 2019, she was an Associate Professor at the Graduate School of Engineering, The University of Tokyo, where she is currently a Professor. Her research interests include medical robotics, surgical navigation systems, and biomedical instrumentation. She is a member of the International Society for Computer Aided Surgery, Japan Society of Computer Aided Surgery, and Japanese Society for Medical and Biological Engineering.

Kazuaki Hara received the B.S., M.S., and Ph.D. degrees in precision machinery engineering from The University of Tokyo, Tokyo, Japan, in 2014, 2016, and 2020, respectively.

He was a Project Researcher at the Medical Device Development and Regulation Research Center, The University of Tokyo, from 2020 to 2022. He was a Project Assistant Professor at The University of Tokyo Hospital, Tokyo, from 2022 to 2023, where he is currently an Academic Specialist. His research interests include medical robotics, automated surgery, and intra-operative measurement.

IEEE Transactions on Automation Science and Engineering (T-ASE) paper, presented at ICRA 2026, Vienna, Austria.

Junchen Wang received the B.E. and Ph.D. degrees in mechanical engineering from Beihang University, Beijing, China, in 2006 and 2012, respectively.

From 2012 to 2016, he was a Post-Doctoral Research Fellow with The University of Tokyo, Tokyo, Japan. Since 2016, he has been an Associate Professor with Beihang University. His research interests include surgical robotics, medical image computing, and surgical navigation.

Ken Masamune received the B.S., M.S., and Ph.D. degrees in precision machinery engineering from The University of Tokyo, Tokyo, Japan, in 1993, 1995, and 1999, respectively.

From 2000 to 2005, he was a Lecturer and an Associate Professor at Tokyo Denki University. From 2005 to 2014, he was an Associate Professor at the Graduate School of Information Science and Technology, The University of Tokyo. He is currently a Full Professor with the Faculty of Advanced Techno Surgery (FATS), Advanced Biomedical Engineering and Sciences, Tokyo Women's Medical University, and a Visiting Professor with Waseda University, Joint Graduate School of Tokyo Women's Medical University and Waseda University, Cooperative Major in Advanced Biomedical Sciences. His research interests include medical robotics, mixed reality, clinical information systems in medicine, and medical device regulatory sciences. He is a Board Member of the International Society for Computer Aided Surgery, Japan Society of Computer Aided Surgery, Robotics Society of Japan, and the Society for Nursing Science and Engineering.

Hideyuki Suenaga received the Ph.D. degree in medical science from The University of Tokyo, Tokyo, Japan, in 2004.

He is currently a Lecturer at the Department of Oral-Maxillofacial Surgery and Orthodontics, The University of Tokyo Hospital, Tokyo. His research interests include computer-aided surgery, especially medical devices for surgery.

Yubo Fan (Member, IEEE) received the B.S. degree in mechanics from Peking University, Beijing, China, in 1987, and the Ph.D. degree in biomechanics from Sichuan University in 1992.

He joined as a Faculty Member at Sichuan University in 1992. He served as the Chair for the School of Architecture and Environment from 2002 to 2005. He is currently a Professor and the Dean of the School of Engineering Medicine, Beihang University, Beijing. He has published more than 300 research articles, being the Elsevier Highly Cited Scholar in Biomedical Engineering with an H-index of 80. His research interests include biomechanics, rehabilitation engineering, and medical robotics. He was the President of Chinese Society of Biomedical Engineering from 2008 to 2015. He is the President-Elect of the World Association for Chinese Biomedical Engineers, an Executive Committee Member of the International Federation for Medical and Biological Engineering, a Council Member of the World Council of Biomechanics, and the Director of the Key Laboratory for Biomechanics and Mechanobiology, Chinese Ministry of Education.